Int. J. Electrochem. Sci., 10 **(2015)** 5488 - 5497

International Journal of
ELECTROCHEMICAL
SCIENCE
www.electrochemsci.org

Arc Vapour Deposition of Iron Film during Magnetron Sputtering of Ti Film: Effect of Substrate's Materials and Surface Roughness

Kok-Tee Lau[1,*], *Zurianee Lokman Loganathan*[1], *R. Abd-Shukor*[2]

[1]Faculty of Manufacturing Engineering, Universiti Teknikal Malaysia Melaka, 76100 Durian Tunggal, Melaka, Malaysia
[2]School of Applied Physics, Universiti Kebangsaan Malaysia, 43600 Bangi, Selangor, Malaysia
[*]E-mail: ktlau@utem.edu.my

Received: 2 March 2015 / *Accepted:* 29 April 2015 / *Published:* 27 May 2015

Arcing of non-target surface is the main contamination cause of sputtering process, which could be minimized through the effective control of the deposition parameters. However, there is an insufficient understanding of the arc vapour deposition's role to the film contamination during magnetron sputtering process, particularly on different substrate's materials and surface roughnesses. Thus, the current paper investigates the arc vapour deposition of ionized iron atom contaminants on the conductive and nonconductive substrates with different surface roughnesses during the magnetron sputter deposition process. The electric arcing occurred on substrate holder was triggered by the electric short-circuit between the supposedly electrically isolated substrate holder and adjacent metallic components. Energy dispersive X-ray spectroscopy and X-ray diffraction indicate that all the deposited films composed of iron (α-ferrite) as the dominant element, with Ti as the minor element. Scanning electron microscopy shows thicker iron films were deposited on the conductive aluminium and mild-steel substrates, in comparison to the film deposited on the nonconductive glass substrate. Field-emission scanning electron microscopy displayed columnar structure for the iron films. The variation in film thickness between the conductive and nonconductive substrates can be explained by the following mechanism: (i) stronger Coulombic attractions of the incoming ionized Fe atoms to the larger electric field generated by conductive substrate, and/or (ii) stronger Coulombic repulsion of the incoming ionized Fe atoms by the deposited Fe ions trapped on nonconductive substrate due to poor electrical grounding. Thus, substrate's material and surface roughness are the determining factors controlling the deposition rate of ionized iron atoms onto the substrate during the arc vapour deposition process.

Keywords: Substrate's Resistivity; Contamination Control, Voltage-biased Substrate; Electrical Grounding; Ion Deposition; Coulombic attraction and repulsion.

1. INTRODUCTION

Sputtering deposition technique has been widely used to deposit high quality metallic film, such as titanium [1], gold [2], and iron [3] metal films for the catalysis, biomedical and microelectronics applications. The deposition process involves physical vapourization of atoms from a solid target surface due to bombardments from the energetic ionic atomic-sized particles in a low pressure gas (plasma) environments [4]. Specifically, the operation of a commonly used magnetron sputtering configuration involves electrons and Ar atoms confinements in the form of plasma near to the sputtering target's surface for reproducible, stable and long-lived sputter atoms vapourization [4]. The sputtering technique offers several advantages such as capability to deposit any coating materials, stable and long-lived vapourization source, and etc [4]. Nevertheless, this technique encounters contamination problems which are caused by, among others, outgassing from target, processing gas impurity and arcing of non-target surface [4].

The contaminations caused by arcing of non-target surface during sputtering process could be minimized through the effective control of the deposition parameters [4]. These controls in turn avoid acquiring new equipment set-up or modification that incurs higher operation cost. Previous study reported five main factors that influence the properties of sputter deposited film, that are substrate's bias voltage, sputtering power, substrate temperature, and distance between substrate and target [4, 5]. It is believed that the voltage-biased substrate's surface interacts significantly with the incoming ionized atoms, particularly ions from the contaminating arcing process, which in turns controlling the film's deposition rate and chemical composition [5]. Nevertheless, there is insufficient understanding of the influence of substrate's material and surface roughness on deposited film contaminated by arc vapour deposition, during the magnetron sputter deposition process. Studies on the interaction mechanism between the substrate and incoming ionized atoms are limited [4, 6] and this may be due to the current design of experiment approach, which focused more on the sputter deposition parameter optimization for the similar substrate materials, with the intention to decrease optimization cost and time [5].

The current paper reports the effect of substrate's materials and surface roughness on the film deposition caused by arc vapour deposition, occurred in concurrent with the magnetron sputter deposition processes. Film's thickness and microstructural characterizations were conducted by means of scanning electron microscopy (SEM) and field-emission scanning electron microscopy (FESEM). Elemental and phase compositional study of the deposited film were conducted using energy dispersive X-ray spectroscopy (EDS) and X-ray diffraction (XRD). These characterization findings intend to shed light on the deposition mechanism corresponds to the arc vapour deposition on the voltage-biased substrates.

2. MATERIALS AND EXPERIMENTS

Rectangular-shaped substrate materials with identical planar surface area were cut from soda-lime glass slide (Ship Brand, China), mild steel sheet (CSC Steel Holding, Malaysia) and pure

aluminium sheets (Aluminium Company of Malaysia Bhd). After cleaned by ultrasonication in acetone for 30 mins and then air-dried, the substrates were fixed by steel clamps onto the vertical shafts of turn-able substrate holder of the physical vapour deposition (PVD) equipment. Film deposition using the unbalanced close field direct-current PVD magnetron sputtering system (Model: VTC PVD-1000, Korea VAC-TEC Co. Ltd., South Korea) was operated using two vertically mounted titanium (Ti) target (Ti purity = 99.99 wt%, dimensions in mm = 600×100×30, Korea VAC-TEC Co. Ltd., South Korea) in Argon gas flow environment (purity = 99.9 vol%, L'Air Liquide S.A.) containing low oxygen impurities (i.e., O_2 and H_2O). More details of parameter settings used during the deposition process are in Table 1.

Table 1. Parameter settings used in film deposition by the DC magnetron sputtering process

Parameter Settings	Process Stages		
	Stage 1: Ion Cleaning	Stage 2: Film Deposition	Stage 3: Cooling
Sputtering Power (W)	0	3000	0
Target Shutter Status	Closed	Opened	Closed
Vacuum Pressure (mbar)	5.0×10^{-3}	5.0×10^{-3}	5.0×10^{-3}
Argon Gas Flow Rate (sccm)	180	200	200
Substrate Bias (V)	-220	-220	-220
Duration (min)	30	60	30
Substrate Temperature (°C)	300	300	300 to 25
Substrate Planetary Rotation Speed (rev/min)	2	2	2

Deposited films were characterized using Scanning Electron Microscope (SEM, 15 kV accelerating voltage, secondary electron emission mode, Model: Evo 50, Carl Zeis AG). In addition, thicknesses of the deposited films were determined by ImageJ software on the captured SEM micrographs of the films' cross-sections, after applying image pixel-scale calibration. Details surface and cross-sectional microstructure characterization of the deposited film on glass substrate was characterized using Field-emission Scanning Electron Microscope (FESEM, 3 kV accelerating voltage, secondary electron emission mode, Model: Merlin compact-60-25, Carl Zeis AG, Germany). Chemical elements in the deposited film were identified using Energy-Dispersive Microanalysis (EDS, Oxford Instrument plc, UK) integrated to the FESEM. Phase composition of the film was investigated using glancing angle X-Ray Diffraction (GAXRD, Cu-Kα1 radiation, wavelength = 0.15406 nm, angle of incidence 1° 2θ, speed 3°/min, step size 0.05° 2θ, Model: X'pert PRO, PANalytical B.V., The Netherlands). Dimensions of the substrate materials were measured using a standard Vernier caliper and micrometer gauge. The surface roughnesses of the substrate were measured using stylus

profilometer (Evaluation distance = 4 mm, Model: SJ-301, Mitutoyo Co.) according to JIS B 0601 (1994) standard.

Table 2. Basic properties of substrate materials

Substrate Materials	Dimensions (length and width ±0.5 mm, thickness ±0.01mm)	Surface Roughness of R_a (µm)	Theoretical Electrical Resistivity (Ω.m)		Film Thickness (µm)
			at 25°C	at 300°C	
Soda-lime Glass	17.0×16.0×1.00	0.02±0.01	5.1×10^{12} [7]	5.9×10^{5} [7]	0.47±0.07
Mild Steel (AISI 1018 grade)	17.0×16.0×0.80	0.42±0.02	16×10^{-8} [8]	68×10^{-8}[8]	2.41±0.20
Aluminium (Purity: 99.9 wt%)	17.0×16.0×0.80	0.62±0.03	2.7×10^{-8} [9]	5.8×10^{-8} [9]	2.31±0.23

3. RESULTS AND DISCUSSION

Topographies and cross-sections of the deposited films on soda-lime glass, steel and aluminium substrate materials are shown as SEM micrographs in Fig. 1.

The three substrates were used as-received from the manufacturers, thus have different surface roughness (Table 2). Glass substrate had the smoothest surface, followed by mild steel and aluminium substrates. Surface microstructures of deposited film appear resembled with the surface microstructure of bare substrates before film deposition. The rough surface microstructures of the film deposited substrates (as observed in SEM topographical view in Fig 1), especially for steel and aluminium substrates suggest film deposition emulated the surface microstructure of the bare substrates. The observations supported previous finding that substrate's surface roughness predominantly influenced the film deposition microstructure [6].

On the other hand, the conductive substrates gave higher film thicknesses (i.e., 2.41±0.20 and 2.31±0.23 µm for the respective film deposited on steel and aluminium substrates) as compared to the nonconductive glass substrate (i.e., 0.47±0.07 µm). The observation implies higher deposition rate of ionized sputtered atoms onto the conductive substrates resulted from stronger interactions of ionized atoms with the electric field formed by negative-biased conductive substrates. Previous study showed 80 and 5 percents of vapourized atoms are ionized atoms during the respective arc vapour and magnetron sputter deposition processes [10]. The current study proposed that the applied voltage bias (which is –220 V) was extended from the substrate clamp (which is attached on the rod of the substrate holder) to the conductive substrate with negligible voltage drop. The negligible voltage drop is expected because of the low resistance of the conductive substrates (see Table 2). A higher resistance

of the nonconductive substrate suggests slightly lower voltage was applied across the glass substrate, thus a lower electric field was generated. This resulted in a weaker ions attraction onto the glass substrate, which gave lower film deposition thickness.

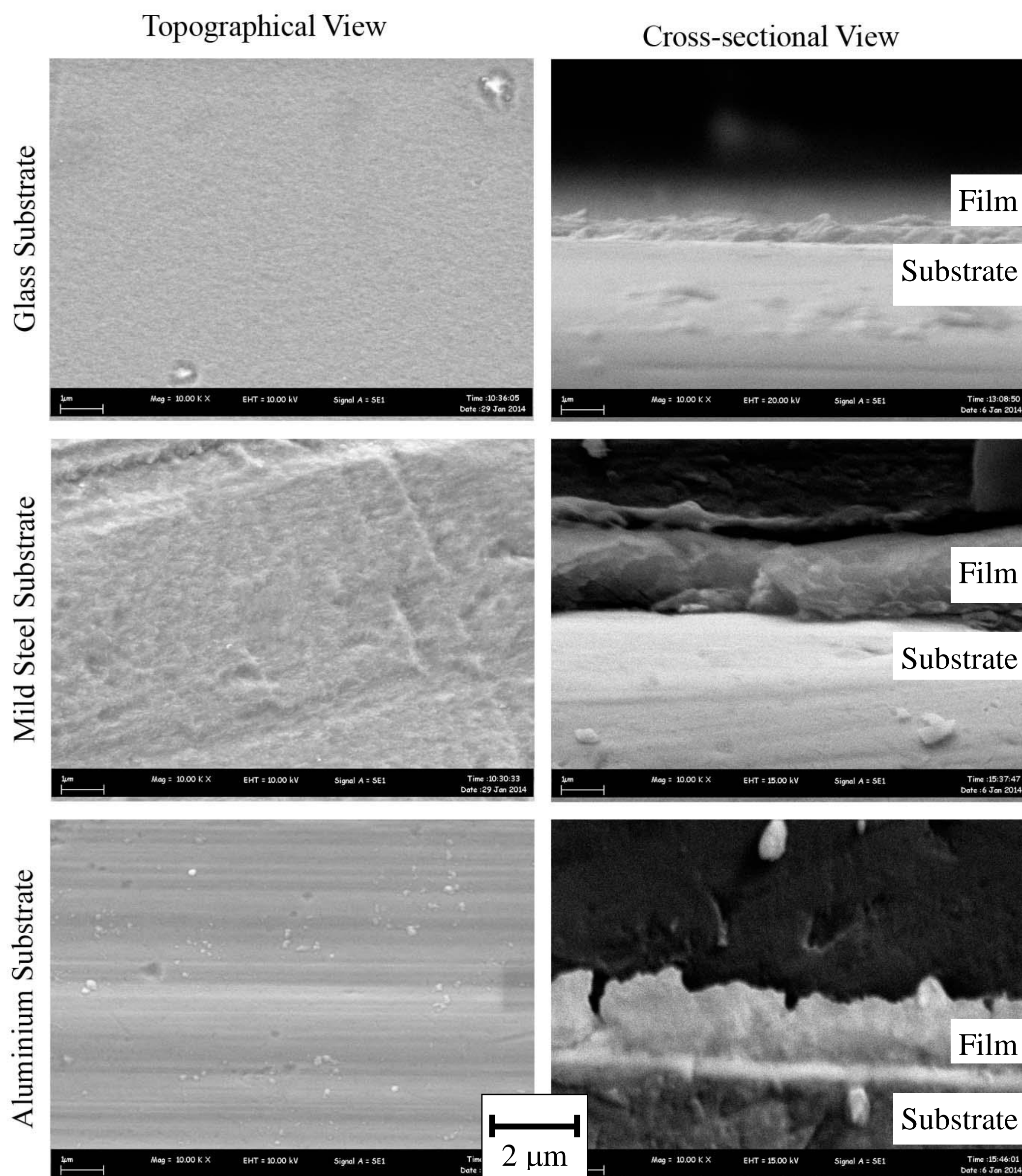

Figure 1. Topographical and cross-sectional view of film deposited on different substrates

Another possible explanation for the lower deposition thickness for glass substrate is due to stronger repulsion of incoming positive-charged ionized atoms by the deposited positive ions accumulated (trapped) [11] on the glass substrate surface, which in turns reduce the deposition rate of the incoming atoms. Higher ion accumulation on the glass substrate surface is expected due to poor substrate's electrical grounding (i.e., discharging or charge elimination process from substrate through the electrical path between the substrate and the ground of magnetron sputtering equipment [4]). It is believed the conductive steel and aluminium substrates have better electrical groundings as compared

to the glass substrate (as implied by their electrical resistivity values in Table 1), thus weaker Coulombic repulsion of these substrates to the incoming ions were resulted. However, electric field generated by the accumulated ions is considered lower than the electric field generated by the voltage-biased substrate, thus weak interaction of the incoming sputtered ions is expected with the accumulated ions. The two proposed ionized atoms deposition mechanisms, which explained a relatively lower deposition rate on the nonconductive substrate as compared to conductive substrates, are illustrated in Fig. 2.

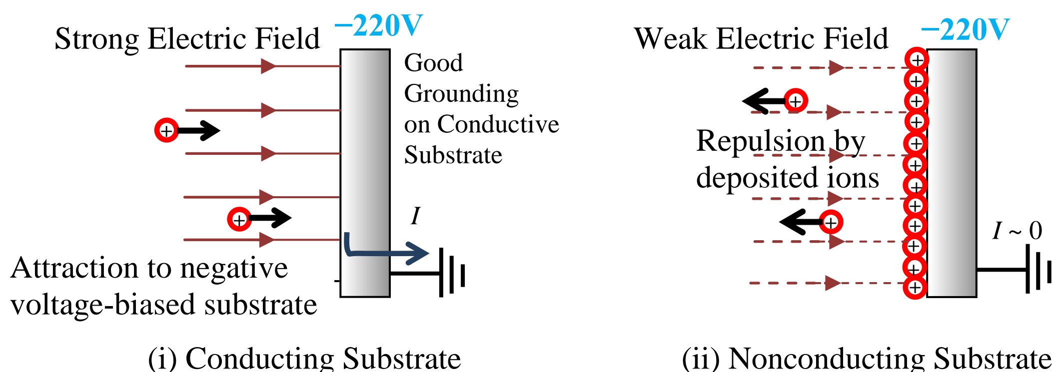

Figure 2. Schematic illustrations of proposed ionized atom deposition mechanisms related to: (i)Conducting Substrate: Strong attraction of ionized atoms with the electric field generated by conductive substrate, and (ii) Nonconducting Substrate: Strong repulsion of incoming ionized atoms by the deposited ions trapped on the nonconductive substrate due to poor electrical grounding

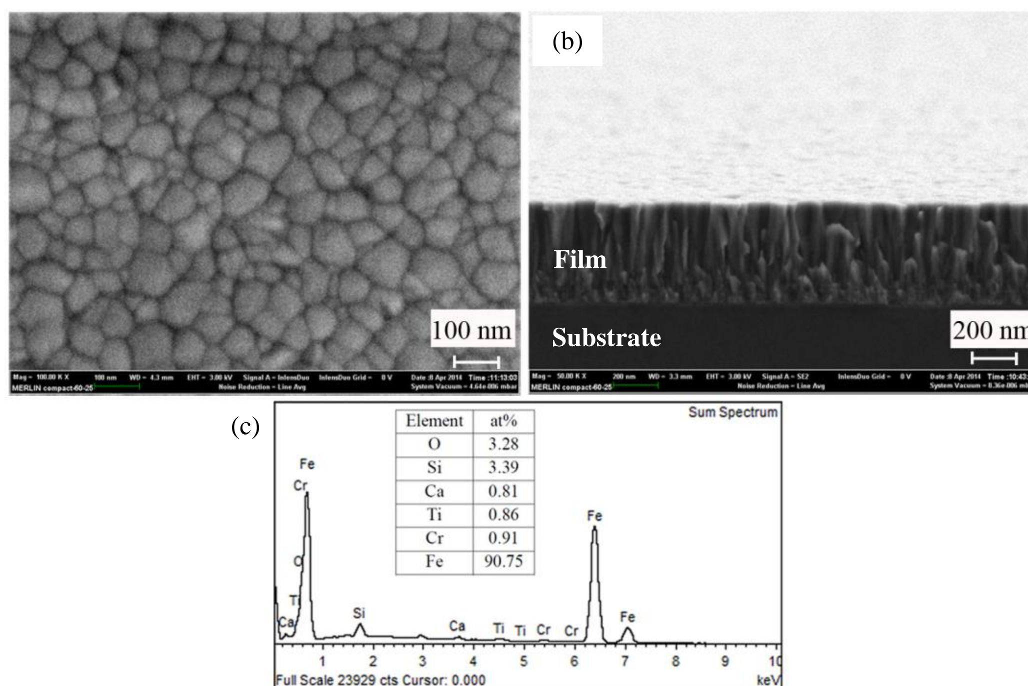

Element	at%
O	3.28
Si	3.39
Ca	0.81
Ti	0.86
Cr	0.91
Fe	90.75

Figure 3. FESEM micrographs of sputtered Fe-rich film on soda-lime glass substrate at: (a) surface, and (b) cross-sectional view. EDS spectrum of the Fe-rich film's surface (inset: chemical compositions of detected elements) is shown in (c)

A higher magnification of the surface microstructure (refer Fig. 3(a)) of film deposited on the soda-lime glass substrate displayed columnar diameter wide range of grain size along the substrate plane. Using the Heyn intercept method [12], the measured mean linear intercept length of the columnar diameter is 60±5 nm. Cross-sectional view (refer Fig. 3(b)) showed the columnar microstructure of the deposited film along the c-axis of the film which is a typical microstructure deposited by PVD [4]. The formed columns were oriented at a tilted angle from the normal of the substrate plane, and are believed to be governed by the shadowing of vapour beam by atoms within the growing film [13].

The EDS spectrum (Fig. 3(c)) shows the presence of Fe as major element in the sputtered film (also labeled as Fe-rich film) deposited on the soda-lime glass substrate, with Ti, Cr, Si and Ca presence as minor elements. The overwhelming concentration of Fe and significant presence of Cr (both elements are believed originated from stainless steel), and surprisingly low Ti concentration (possibly from sputtering of Ti target) strongly indicates that the film was predominantly deposited through other type of deposition mechanism which involved evaporations of Fe and Cr atoms from the substrate holder surface. In addition, the other detected elements were probably originated from the glass substrate. It is unlikely O element is present in the film because deposition was conducted in inert environment, and did not show indication of oxidation (i.e., metallic colour appearance). Following this observation, a subsequent visual inspection on the d.c. magnetron sputtering chamber had detected prominent electrical arc scar on the base and shaft of substrate holders. This finding indicates an accidental arc vapour deposition of Fe and Cr atoms occurred during the operation of the magnetron sputtering, where evaporations of the elements from the substrate holder surface were triggered by the electrical arcing on the surface of substrate holder. Arc vapour deposition is another form of PVD process that utilizes the vapourization from an electrode under arcing conditions (i.e. when high electric current passing through gas or vapour of two closely spaced electrode) as a source of vapourized material [4]. It is proposed by the current study that accidental electrical connections were formed between electrically-isolated conducting components, probably triggered by the presence of metallic film deposition at the very fine gaps between the metallic parts connected to the substrate holder, particularly metallic parts separated by alumina insulating O-rings. The substrate holder was supposedly designed to be electrical-isolated from the other metallic components in the PVD chamber [14].

Evidences which pointed to the occurrence of arc vapour depositions of Fe and Cr atoms further support the proposed ionized atoms deposition mechanism for the current deposited films (see Fig. 3 and related paragraphs). This is because studies showed that vapourized atoms from the arc vapour deposition mechanism produced higher ionized atoms and are responded strongly to substrate's voltage bias [4, 10].

Fig. 4 shows XRD patterns of the iron films deposited on soda-lime glass, mild steel and aluminium (Al) substrate respectively, which supported the SEM and EDS observations, as well as the films' thicknesses data. The XRD patterns were analysed using 'X-Pert High Score' software (PANalytical B.V.), and were indexed using ICDD-JCPDS database. A single peak of deposited film on the glass substrate was detected at ~44.5° as the (110) peak of α-iron (ferrite, highest peak, ICDD No.: 00-006-0696). It is expected that the soda-lime glass does not give any peak because of its

amorphous phase [15]. The relatively broad peak indicates the films had relatively small crystal grain [16], which was supported by the FESEM micrograph in Fig. 3 (a). Furthermore, the α-iron peaks supported the EDS result and confirmed the presence of highly oriented columnar-structured iron film (see Fig. 3(b)) on the substrate.

The films deposited on mild steel and aluminium substrates also gave their respective peaks at ~44.5°, indicates the presence of same phase in the deposited films. A distinct but small aluminium peak was observed for the aluminium substrate (refer to ICDD No.: 01-089-2837). Meanwhile, there were two smaller peaks partially overlapped with the main 44.5° peak for the iron film deposited on mild-steel. It is expected mild-steel substrate has similar XRD pattern with the iron peak [17], but because of the limited X-ray penetration into the substrate, the mild steel substrate's contribution to the observed peaks of iron film is negligible. In addition, crystal lattice distortion of α-iron phase, as indicated by the presence of shoulder peaks [16], was unlikely to occur in the steel substrate because of inert operating environment and low substrate temperature (i.e., 300°C). The distorted iron crystal lattice of the deposited iron film (as illustrated by shoulder of 44.5° peak at lower 2θ position) may be caused by the substitution of Fe atom with larger atomic radii Cr and Ti atoms in the crystal lattice. Where else, a small peak of the film at the higher 2θ value indicates reduction in the lattice spacing, resulted from the strain relaxation of the iron film [18].

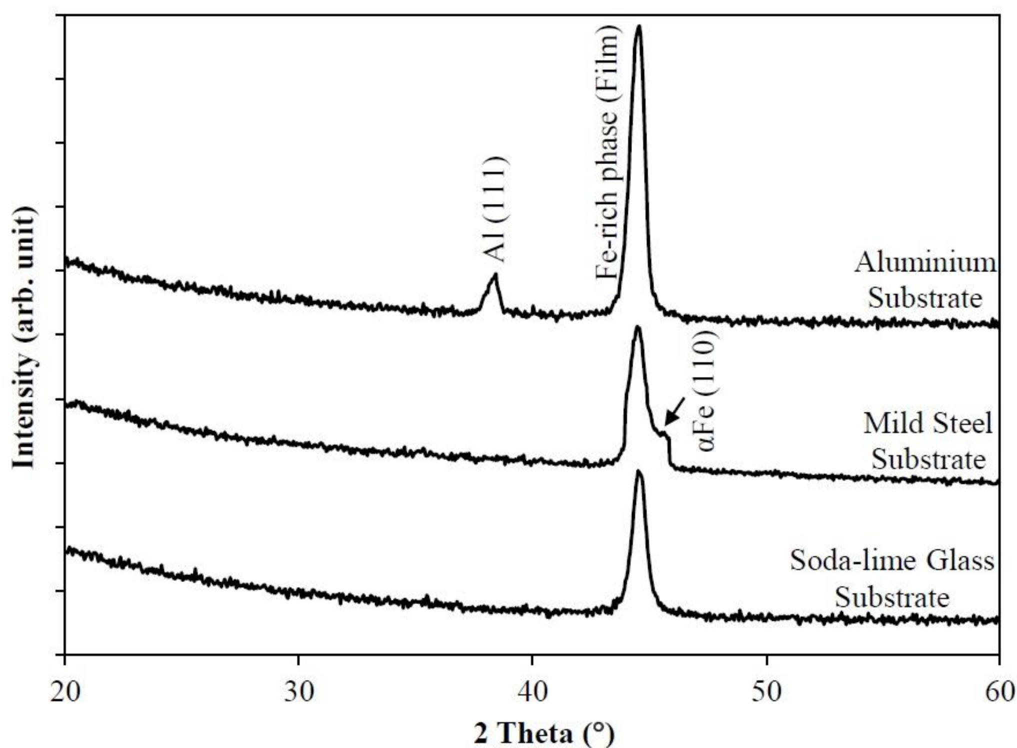

Figure 4. XRD patterns of Fe-rich film deposited on different substrate materials

Iron film deposited on aluminium substrate displayed the highest iron peak intensity at 2θ = 44.5°, twice the peak intensity of iron films deposited on mild steel and glass substrates, with both the latter films had similar peak intensity. The results do not correlate with the film thickness result,

where film deposited on aluminium has nearly same thickness with iron film deposited on steel, but five-times thicker than film deposited on glass (as stated in Table 2). The discrepancy between the XRD peak intensity and thickness value obtained via SEM of the iron peak intensity of film deposited on mild-steel may be due to the deposition of distorted crystal structured iron phase, as indicated by the presence of two small peaks beside the main iron peaks.

4. CONCLUSIONS

Iron (α-ferrite) films were deposited on the respective conductive aluminium and mild-steel substrates and nonconductive soda-lime glass substrate by arc vapour deposition mechanism, during the operation of d.c. magnetron sputtering of Ti target. Electric arcing on the substrate holder was caused by the electric short-circuit between the supposedly electrically isolated substrate holder and other metallic components in the PVD chamber. Ti was detected as minor element, thus indicate magnetron sputtering process of Ti atoms was negated by the high deposition rate of Fe atoms through the arc vapour deposition process. Thicker iron films were deposited on the conductive aluminium and mild-steel substrate, in comparison to the film deposited on the nonconductive glass substrate. The film thickness difference between the conductive and nonconductive substrates can be explained by the following mechanism: (i) stronger Coulombic attraction of the incoming ionized Fe atoms to the low electric field of the nonconductive substrate, and/or (ii) stronger Coulombic repulsion of the incoming ionized Fe atoms to the respective deposited Fe ions on nonconductive substrate due to poor electrical grounding. It is shown that substrate materials and their surface roughness are the determining factors controlling the deposition rate of ionized iron atoms onto the substrate during the arc vapour deposition process. Thus, it is suggested that iron contamination can be minimized (or diminished) by decreasing substrate's voltage bias toward zero bias voltage or set the substrate with opposite polarity voltage for pure deposition of sputtered atoms. The conditions reduce the electric force attraction on the incoming ionized contaminants and decrease the probability of arcing between substrate holder and nearby conductive components that causes the arc vapour deposition of iron films as discussed in the study.

ACKNOWLEDGEMENT
The authors are grateful to the Ministry of Education Malaysia for supporting this work under grant no.: FRGS(RACE)/2012/FKP/SG07/03/1/F00154 and FRGS/2/2013/SGD2/UKM/01/1 and Universiti Kebangsaan Malaysia under grant no. UKM-DPP-2014-055. The authors also acknowledge Morphology Laboratory, Centre for Research and Innovation Management, Universiti Kebangsaan Malaysia for the FESEM characterization service.

References

1. N. Arshi, J. Lu, C. Lee, J. Yoon, B. Koo and F. Ahmed, *Bull. Mater. Sci*. 36 (2013) 807.
2. J. Siegel, O. Lyutakov, V. Rybka, Z. Kolská and V. Švorčík, *Nanoscale Res. Lett*. 6 (2011) 96.
3. A. Iljinas, J. Dudonis, R. Bručas and A. Meškauskas, *Nonlinear Anal. Model. Control*, 10 (2005) 57.

4. D. M. Mattox, *Physical Vapor Deposition (PVD) Processing*. 2nd ed. Elsevier Inc. Kidlington (2010).
5. J. Lin, W. D. Sproul, J. J. Moore, Z. Wu, S. Lee, R. Chistyakov and B. Abraham, *JOM*, 63 (2011) 48.
6. H. Adachi, T. Hata and K. Wasa, Basic Process of Sputtering Deposition, in *Handbook of Sputter Deposition Technology: Fundamentals and Applications for Functional Thin Films*, Nanomaterials, and MEMS, K. Wasa, I. Kanno and H. Kotera, Editors, Elsevier Inc. *Oxford* (2012) 295-359.
7. D. R. Uhlmann, H. K. Bowen and W. Kingery, *Introduction to Ceramics.* John Wiley & Sons Inc. New York (1976) 885.
8. ASM International, Physical Properties of Carbon and Low-Alloy Steels, in *ASM Handbooks*, ASM International: Materials Park (1990) 195.
9. D. R. Lide, ed. *CRC Handbook of Chemistry and Physics*. 73rd ed. CRC Press, Boca Raton (1992) 12.
10. E. Lugscheider, C. Barimani, C. Wolff, S. Guerreiro and G. Doepper, *Surf. Coat. Technol*. 86 (1996) 177.
11. A. E. Wendt and S. B. Wang, *Method and Apparatus for Plasma Processing with Control of Ion Energy Distribution at the Substrates*, United States Patent No. US6201208 B1 (2001).
12. Q. Tang, K. Kikuchi, S. Ogura and A. Macleod, *J. Vacuum Sci. Technol*. A, 17(1999) 3379.
13. A. G. Dirksand and H.J. Leamy, *Thin Solid Films*, 47 (1977) 219.
14. Korea VAC-TEC Co. Ltd., *Operation and Installation Manual: Vacuum PVD System*, Model VTC PVD-1000 Paju (2007).
15. K. Cai, M. Müller, J. Bossert, A. Rechtenbach and K. D. Jandt, *Appl. Surf. Sci.* 250 (2005) 252.
16. B. D. Cullity, *Elements of X-ray diffraction*. 2nd ed. Addison Wesley Publishing (1978).
17. K. T. Lau, *Controlled Surface Layer Deposition for Steel Surface Hardening*, The University of New South Wales (2012).
18. C. Murray, *Diffraction-based analysis of the mechanics of nanoelectronics*, in 2013 CLASSE Seminars. Cornell High Energy Synchrotron Source, Cornell University, Ithaca (2013).

© 2015 The Authors. Published by ESG (www.electrochemsci.org). This article is an open access article distributed under the terms and conditions of the Creative Commons Attribution license (http://creativecommons.org/licenses/by/4.0/).